

Structure-based Optimization of Hydroxylactam as Potent, Cell-Active Inhibitors of Lactate Dehydrogenase

BinQing Wei^{a*}, Kirk Robarge^a, Sharada S. Labadie^a, Jinhua Chen^b, Laura B. Corson^a, Antonio DiPasquale^a, Peter S. Dragovich^a, Charles Eigenbrot^a, Marie Evangelista^a, Benjamin P. Fauber^a, Anna Hitz^a, Rebecca Hong^a, Kwong Wah Lai^b, Wenfeng Liu^b, Shuguang Ma^a, Shiva Malek^a, Thomas O'Brien^a, Jodie Pang^a, David Peterson^a, Laurent Salphati^a, Deepak Sampath^a, Steven Sideris^a, Mark Ultsch^a, Zijin Xu^b, Ivana Yen^a, Dong Yu^b, Qin Yue^a, Aihe Zhou^a, Hans E. Purkey^{a*}

^aGenentech, Inc., 1 DNA Way, South San Francisco, CA 94080, USA

^bWuXi AppTec, 288 Fute Zhong Road, Waigaoqiao Free Trade Zone, Shanghai, 200131, China

* Correspondence: Wei.BinQing@gene.com , Purkey.Hans@gene.com

ABSTRACT

Structure-based design was utilized to optimize 6,6-diaryl substituted dihydropyrone and hydroxylactam to obtain inhibitors of lactate dehydrogenase (LDH) with low nanomolar biochemical and single-digit micromolar cellular potencies. Surprisingly the replacement of a phenyl with a pyridyl moiety in the chemical structure revealed a new binding mode for the inhibitors with subtle conformational change of the LDHA active site. This led to the identification

of a potent, cell-active hydroxylactam inhibitor exhibiting an in vivo pharmacokinetic profile suitable for mouse tumor xenograft study.

KEYWORDS: lactate dehydrogenase, tumor metabolism, glycolysis, X-ray crystal structure, structure-based design

A hallmark of cancer cells' dysregulated metabolism is the dependence on the conversion of glucose to lactate to generate energy under normal oxygen conditions, a process termed aerobic glycolysis (i.e. Warburg effect). This is in stark contrast to the mitochondrial tricarboxylic acid cycle utilized by normal cells. Lactate dehydrogenase A (LDHA) is a key enzyme that catalyze the final step in the glycolytic pathway, reducing pyruvate to lactate and regenerating NAD⁺ equivalents necessary for continued glycolysis. Overexpression of LDHA is found in many types of cancer cells and has been correlated with poor clinical outcome.¹ Inhibition of the enzyme activity by knockdown or silencing of the LDHA gene has been shown to reduce cancer cell growth in vitro under hypoxic conditions and to suppress tumor growth in xenograft models.² Together these data underscore the therapeutic potential of LDHA inhibition for the treatment of cancer. Recently, the lactate dehydrogenase B isoform (LDHB) has been found to control lysosomal activity and autophagy in cancer cells³ and to be an essential gene for triple-negative breast cancer.⁴ These findings led us to pursue a pan-LDH inhibitor in order to maximize potential efficacy across the broadest set of tumors.

Significant progress has been made in the discovery of LDH inhibitors displaying remarkable enzymatic potency.⁵ However, cellular activity has proved very challenging to obtain. To our knowledge only a few series of cell-active LDH inhibitors have been published to date.⁶⁻⁹ Two of those were shown to reduce lactate level in vivo^{10,11} but anti-tumor efficacy remains

elusive. The high abundance of cellular LDH protein as well as the highly hydrophilic nature of its catalytic site presents significant obstacles to the development of inhibitors suitable for *in vivo* testing. From high-throughput screen of corporate chemical library, we discovered a family of 1,3-dicarbonyl and related dihydropyrone, hydroxylactam compounds that bind LDHA in an NADH uncompetitive manner.¹²⁻¹⁴ Structure and property-based optimization led to the identification of our first cell-active hydroxylactam molecule.⁷ Upon oral dosing in a mice xenograft tumor model, the compound failed to show efficacy, which we hypothesized to result from a relative short half-life and thus insufficient target coverage.¹⁰ Here we report the structure-guided optimization of 6,6-diaryl substituted dihydropyrone and hydroxylactam inhibitors. Unexpectedly, a new binding pose of the chemical series was observed where the diaryl moieties occupying different pockets compared to our previous discovery⁷, This led to the identification of new LDH inhibitors with low nanomolar biochemical and single-digit micromolar cellular potencies, and the resulting impact on *in vivo* pharmacokinetics and efficacy are reported.

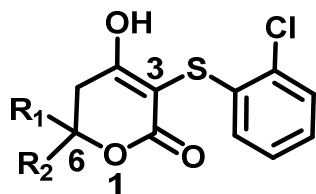
First we searched for optimal diaryl substitutions at the 6-position of the pyrone scaffold, which in terms of enzymatic potency was found to exhibit parallel SAR trends as the hydroxylactam series⁷ but is synthetically more accessible (Table 1). When the two aryl substituents are different, unless specified otherwise, we separated the enantiomers and assayed them individually. IC₅₀ values of the less potent stereoisomers are shown in parentheses. For select molecules, absolute stereochemistry was determined using small molecule crystallography. When the substituents were both 6-membered aryl or heteroaryl cycles, there was no significant difference in their potencies (compounds **1**, **2**, and **4**). In contrast, when a 5-membered heteroaryl was combined with a 6-membered ring, the potency improved by 5 to 11-fold for LDHA (**5**, **7**, **9**, and **11** vs. **1**). A similar trend was observed for LDHB albeit LDHB IC₅₀ values were typically 2

to 6-fold higher than those for LDHA. A combination of two 5-membered heteroaryl cycles did not improve the activity further (**13** vs. **5**). These data suggest that either the axial or the equatorial position prefers a smaller, 5-membered ring when the molecule is bound to LDHA. Conformational analysis of **5** using quantum mechanics showed that in water the thiophen-3-yl moiety slightly prefers axial over equatorial presumably due to lower steric strain (conformational energy difference = 0.2 kcal/mol, Supplemental Materials, Figure S1). However, it is possible that this weak preference may be altered in the protein-bound state.

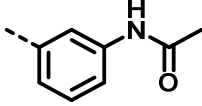
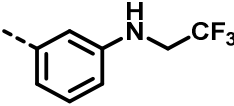
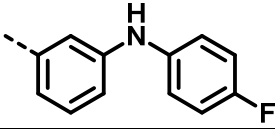
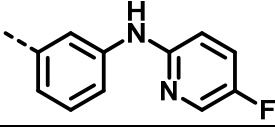
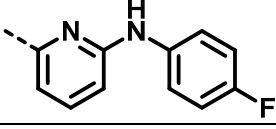
Next, we tried to improve the affinity by exploring substitutions on the 6-membered aryl ring presumably at the equatorial position. Interestingly, the replacement of a phenyl with a 2-hydroxyphenyl improved the potency by 40-fold (**14** vs. **1**). To understand what may have contributed to the potency gain, we solved a cocrystal structure of **14** bound to LDHA at 2.0Å resolution. As shown in Figure 1A, the dihydropyrone core maintained the same NADH uncompetitive binding model as previously observed for this series.¹³ The observed planar geometry of the 3-position carbon was consistent with the expected enol tautomer state. We previously showed that the enol was acidic ($pK_a = 2.4^{13}$) so it was ionized in the structure at a neutral condition. Based on the proximity of hydrogen bonding residues nearby, we inferred that the ester carbonyl bound with the catalytic residue Arg168 while the enolate oxygen bound with both His192 and Asn137 through hydrogen bonds. Although the stereochemistry of **14** was not determined, the chirality of a subsequent analog (**26**) was assigned by small molecule crystallography which supported our assumption (vide infra). The phenyl substituent at the 6-position was found axial, occupying a hydrophobic pocket capped by Tyr238 sidechain and forming an edge-to-face interaction with the 2-chlorothiophenyl moiety of the inhibitor, while the bulkier 2-hydroxyphenyl substituent was equatorial. Replacement of the axial phenyl group with

thiophen-3-yl led to a 12-fold gain (**16** vs. **14**), consistent with the trend observed from simple diaryl compounds (cf. 10-fold gain from **1** to **5**). A water molecule was seen 2.9Å away from the oxygen atom of 2-hydroxyphenyl. Water molecules were observed at almost the same position in two previously published inhibitor-bound structures (PDB entries 4R68 and 5IXS). At this conserved hydration site, water appeared to bind with Thr247 and NADH (Figure 1a) through hydrogen bonds. We hypothesized that the affinity gain of **14** vs. **1** could be attributed to the hydroxyl group serving as a hydrogen bond donor to this conserved water. Substituting a fluorine atom for the hydroxyl reduced the affinity of **16** by 100-fold, to a level close to that of **5**, which supported our hypothesis. Instead of engaging the water, we wondered if further improvement from **16** can be obtained by replacing this water. Computational assessment using WaterMap™ (Schrodinger, version 2015) predicted that this water would be energetically unfavorable to remove due to its multiple hydrogen bond interactions (Supplemental Materials, Figure S2). To test that, the 2-hydroxyphenyl was replaced with 3-aminophenyl (**20** and **22**) and a cocrystal structure of **20** bound to LDHA was determined by X-ray crystallography at 2.1Å resolution. As predicted by modeling, the amino group was observed at the same location where the water used to be and apparently served as a hydrogen bond donor to both Thr247 and NADH (Figure 1B). Compounds **20** and **22** showed a 5 to 6-fold reduction in potency compared to **16** and **14**, respectively, confirming the computational prediction.

Table 1. Structure-Activity Relationship for 6,6-Diaryl Substituted Dihydropyrones.



Ex	R ₁	R ₂	LDHA IC ₅₀ ¹ (μM)	LDHB IC ₅₀ ¹ (μM)
1	phenyl	phenyl	1.0±0.3	3.1±0.1
2 (3)	pyridin-2-yl	phenyl	0.92±0.28 (2.4±0.7)	4.7±0.2 (19±3)

4	pyridin-2-yl	pyridin-2-yl	1.2±0.2	2.9±0.2
5 (6)	thiophen-3-yl	phenyl	0.09±0.02 (0.43±0.21)	0.2±0.07 (0.75±0.2)
7 (8)	thiophen-2-yl	phenyl	0.12±0.01 (0.22±0.02)	1.3±0.1 (1.5±0.2)
9 (10)	thiazol-4-yl	phenyl	0.18±0.01 (1.1±0.1)	0.55±0.01 (2.8±0.1)
11 (12)	thiophen-3-yl	pyridin-2-yl	0.13±0.04 (0.97±0.14)	0.54±0.07 (3.2±0.5)
13	thiophen-2-yl	thiophen-2-yl	0.09±0.01	0.81±0.09
14 (15)	phenyl	2-hydroxyphenyl	0.026±0.004 (0.43±0.17)	0.075±0.009 (0.95±0.18)
16 (17)	thiophen-3-yl	2-hydroxyphenyl	0.0022±0.0001 (0.022±0.004)	0.015±0.004 (0.09±0.02)
18 (19)	thiophen-3-yl	2-fluorophenyl	0.22±0.02 (0.45±0.03)	0.6±0.1 (0.6±0.1)
20 (21)	thiophen-3-yl	3-aminophenyl	0.013±0.004 (0.19±0.02)	0.0089±0.004 (0.31±0.03)
22 (23)	phenyl	3-aminophenyl	0.13±0.07 (0.45±0.23)	0.25±0.16 (3.8±0.44)
24 ²	thiophen-3-yl		0.043±0.007	0.29±0.03
25 ²	thiophen-3-yl		0.066±0.013	0.4±0.1
26-R (27-S)	thiophen-3-yl		0.004±0.001 (0.036±0.018)	0.047±0.011 (0.075±0.007)
28 (29)	thiophen-3-yl		0.0029±0.0001 (0.063±0.023)	0.065±0.004 (0.33±0.19)
30 (31)	thiophen-3-yl		0.0029±0.0007 (0.0069±0.001)	0.017±0.004 (0.068±0.033)

¹LDHA and LDHB enzymatic assay values are the geometric mean of at least two separate experiments as previously described.¹² ²Racemic mixture was used in the assay.

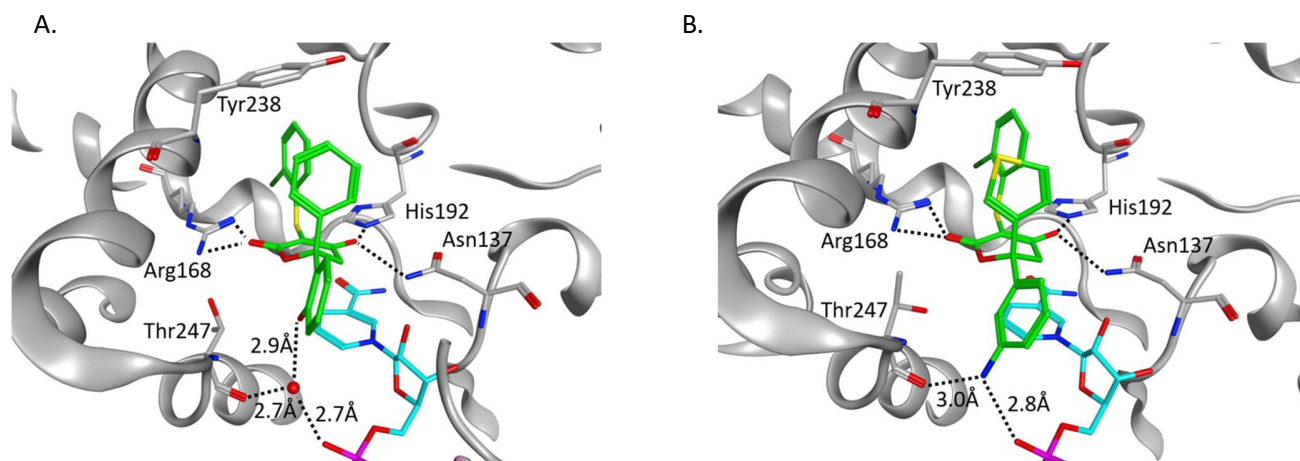


Figure 1. Cocystal structures of LDHA in complex with compound **14** (A, PDB code 6MV8) or **20** (B, PDB code 6MVA). Hydrogen bonds are shown as dashed lines.

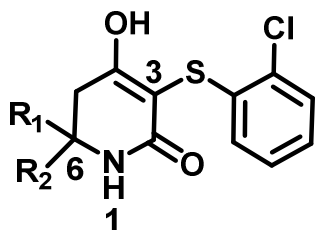
After exploring the polar, confined cavity near the cofactor NADH, we turned our focus to the more solvent-exposed space between Ile241 sidechain and the loop spanning from Gln99 to Arg105 where we previously observed opportunities for hydrophobic interactions.^{13,14} Based on modeling, we made a set of substitutions with increasing size and hydrophobicity off the 3-aminophenyl group of **20** (Table 1). While the smaller, acetyl or 2,2,2-trifluoroethyl moieties showed no improvement, a 4-fluorophenyl or 5-fluoropyridin-2-yl group increased the affinity by 3 to 4-fold (**26** and **28** vs. **20**). A cocrystal structure of **26** bound to LDHA was determined by X-ray crystallography at 2.1 Å resolution (Figure 2A). The binding pose of **26** was similar to that of **20** with the thiophene ring in the axial position. The dihydropyrone core moved slightly away from the cofactor nicotinamide moiety and closer to Tyr238 sidechain, while the 3-(4-fluorophenyl)amino phenyl moiety was “sandwiched” between Ile241 and Gln99 sidechains. Instead of engaging or replacing the conserved water, which remained present, the aniline nitrogen atom was within hydrogen-bond distance from the backbone carbonyl oxygen of Gln99. We determined the stereochemistry of **26** to be R by small molecule X-ray crystallography (Figure S1), which supported the assumed orientation of the dihydropyrone core in the structures of **14** and **20** (Figure 1A and B). Notably, for most of the enantiomeric pairs (Tables 1), one enantiomer was markedly more potent against LDHA than the other enantiomer. This trend appeared even more prominent as the binding affinity was improved (cf. **14-21**, **26-29**). Surprisingly, when the equatorial phenyl of **26** was replaced with a pyridin-2-yl, both enantiomers were equipotent (**30** vs. **31**). This seemed to suggest that the previously weaker enantiomer may bind differently in the case of a thiophen-3-yl and pyridin-2-yl combination. The cocrystal structure of **30** in complex with LDHA (Figure 2B, 2.4 Å resolution) indeed confirmed that the ligand adopted a new pose

compared to **20** and **26**: the thiophen-3-yl moiety became equatorial while the pyridin-2-yl axial. The 4-fluorophenyl substituent on the 6-amino-pyridin-2-yl moiety occupied a hydrophobic pocket surrounded by Pro138 and Leu108 sidechains, which adopted similar conformations as seen in a previous report (PDB entry 4R68).¹⁴

Having optimized biochemical potency in the synthetically more accessible dihydropyrone series, we next switched to the hydroxylactam core, which was shown to have better physicochemical and pharmacokinetic properties than dihydropyrones: lower in acidity ($pK_a = 4.1^{13}$) and plasma protein binding and higher in membrane permeability.^{7,13} The pair of enantiomers **32** and **33** (Table 2) were similar in both absolute and relative LDHA activities compared to their dihydropyrone counterparts **30** and **31**. The stereochemistry of **33** was determined as S by small molecule X-ray crystallography (Figure S2). The cocrystal structure of **32** (Figure 2C, 2.4Å resolution, R enantiomer), bound to LDHA showed that the hydroxylactam core adopted the same pose as previously observed (PDB entry 4ZVV⁷): the amide oxygen atom made H-bond interactions with the Arg168 residue while the enolate oxygen atom with His192 and Asn137. Like its dihydropyrone analog **30**, **32** bound to LDHA with the thiophen-3-yl group equatorial while the 6-((4-fluorophenyl)amino)-pyridin-2-yl moiety axial and filling a hydrophobic pocket surrounded by Pro138 and Leu108. Addition of a second fluorine atom on the phenyl ring did not significantly change the absolute or relative potencies of the enantiomers (**34** and **35**). In contrast, replacement of the 4-fluorophenyl with a cyclohexyl or tetrahydropyranyl reduced the potency of the less active enantiomer by over 10 fold, restoring a marked enantiomeric difference in activity (**36** – **39**) seen among many dihydropyrones (e.g. **26** and **27**). Smaller alkyl (**40** and **41**) and homologated 4-fluorobenzyl (**42** and **43**) substitutions also showed a similar enantiomeric difference. The structures of the dihydropyrone molecule **30** and its hydroxylactam

counterpart **32** together revealed that, on both cores, a new binding pose existed for certain compounds with a thiophen-3-yl and a pyridin-2-yl substitutions at 6-position: the thiophen-3-yl became equatorial in the bound state instead of axial as observed previously (Figure 2A, and PDB entries 4R68 and 4ZVV). We hypothesized that, when two enantiomers were able to adopt different poses in terms of axial-equatorial configuration (Figure 2A and 2B), their core scaffold could always maintain the preferred orientation (i.e. the carbonyl oxygen bound to Arg168 while the enolate oxygen bound to His192 and Asn137 through hydrogen bonds), resulting in the phenotype of equivalent potencies between the stereoisomers. The pyridin-2-yl moiety appeared required for equipotency of enantiomers since the phenyl version behaved differently (**30** and **31** vs. **26** and **27**). Yet the pyridin-2-yl moiety alone was not sufficient as the non-substituted ones showed marked enantiomeric difference (**30** and **31** vs. **11** and **12**). Appropriate aryl substitutions seemed also required, presumably to fulfill the hydrophobic pocket near Pro138 sidechain. Consistent with our hypothesis, replacement of the (4-fluorophenyl)amino moiety with a phenoxy group such as in **44-45** maintained the enantiomeric equipotency while the bulkier quinolin5-yloxy substitution did not (**46-47**). In a previous report on the hydroxylactam series we identified a 4-morpholinophenyl moiety to be a potent equatorial substitution at the 6-position.⁷ So we wondered if substituting it for the equatorial thiophen-3-yl could further improve the potencies. As shown in Table 2, that was not the case (**48** vs **32**, and **50** vs. **44**).

Table 2. Structure-Activity Relationship for 6,6-Diaryl Substituted Hydroxylactams.



Ex	R1	R2	LDHA IC ₅₀ (μ M)	LDHB IC ₅₀ (μ M)	Measured LogD ^a	MiaPaca2 Cell Lactate IC ₅₀ (μ M) ^a	
32-R (33-S)			0.0016 \pm 0.0009 (0.0037 \pm 0.0012)	0.0098 \pm 0.0013 (0.046 \pm 0.012)	2.2	2.0 \pm 0.9	
34 (35)			0.0009 \pm 0.0003 (0.0044 \pm 0.0022)	0.0028 \pm 0.0006 (0.031 \pm 0.009)	2.6	2.2 \pm 0.9	
36 (37)			0.0027 \pm 0.003 (0.055 \pm 0.004)	0.0082 \pm 0.0007 (0.33 \pm 0.01)	2.4	7.2 \pm 0.3	
38 (39)			0.01 \pm 0.001 (0.075 \pm 0.002)	0.034 \pm 0.017 (0.29 \pm 0.12)	1.1	9.1 \pm 1.7	
40 (41)			0.013 \pm 0.006 (0.19 \pm 0.03)	0.17 \pm 0.03 (1.8 \pm 0.05)	ND ^b	ND ^b	
42 (43)			0.0086 \pm 0.0016 (0.16 \pm 0.02)	0.057 \pm 0.016 (0.81 \pm 0.21)	2.5	ND ^b	
44 (45)			0.0025 \pm 0.0004 (0.0032 \pm 0.0004)	0.0095 \pm 0.0024 (0.09 \pm 0.01)	2.6	5.3 \pm 0.9	
46 (47)			0.0038 \pm 0.0016 (0.068 \pm 0.035)	0.025 \pm 0.009 (0.65 \pm 0.2)	2.2	3.6 \pm 0.14	
48 (49)				0.0025 \pm 0.0016 (0.011 \pm 0.004)	0.0017 \pm 0.0012 (0.038 \pm 0.027)	2.0	ND ^b
50 (51)				0.0018 \pm 0.0011 (0.037 \pm 0.007)	0.0022 \pm 0.0012 (0.085 \pm 0.024)	1.9	1.7 \pm 1

^aThe more potent enantiomers were measured. ^b Not determined. MiaPaca2 cell assay values are the geometric mean of at least 2 separate runs as described previously.¹⁴

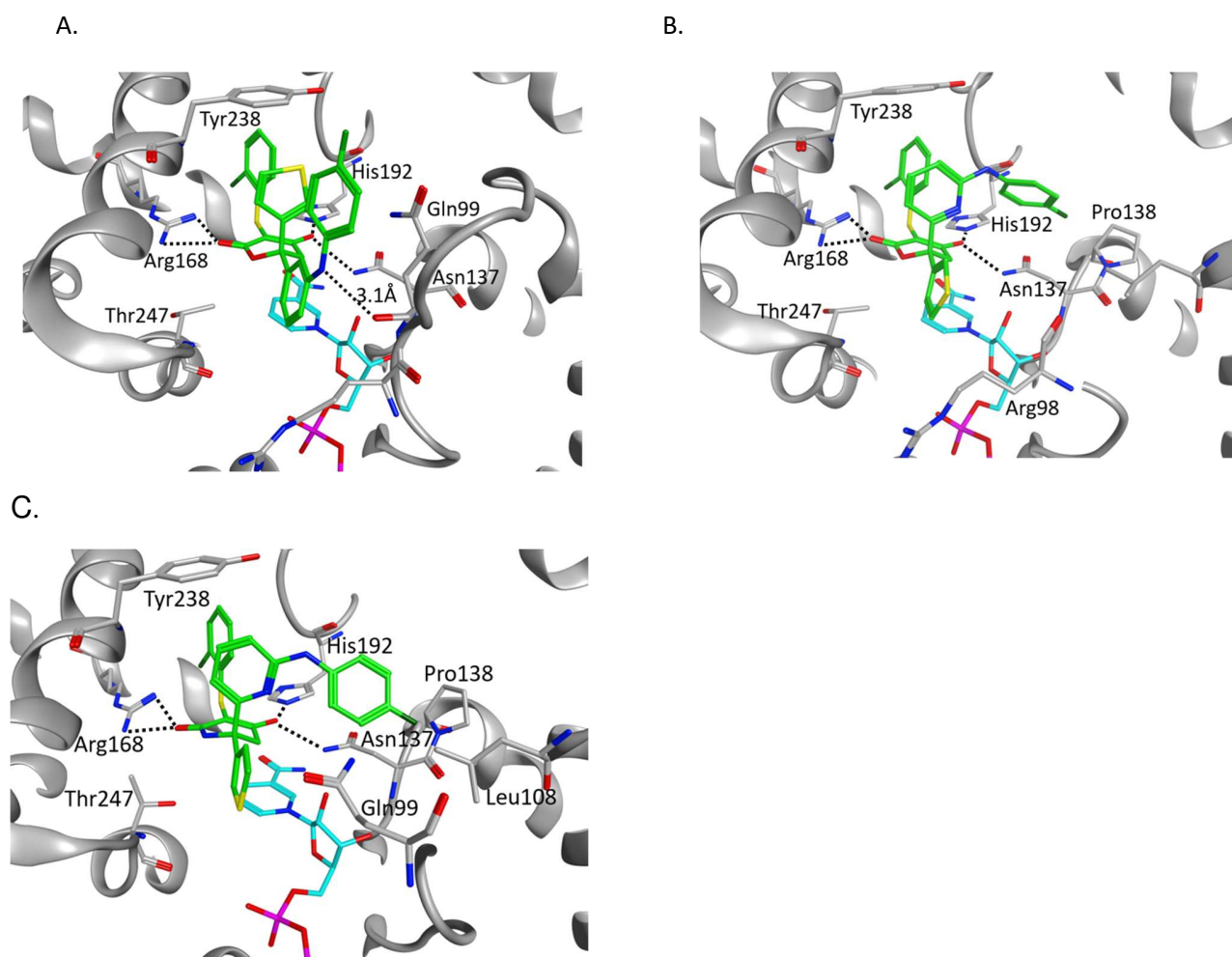


Figure 2. Cocystal structures of LDHA in complex with compound **26** (A, PDB code 6BAD), **30** (B, PDB code 6BB3), or **32** (C, PDB code 6BAG). Hydrogen bonds are shown as dashed lines.

Encouraged by their enzymatic potency, we tested the more active hydroxylactam inhibitors in a MiaPaca2 cell line for the inhibition of lactate production (Table 2, **32**, **34**, **36**, **38**, **44**, **46**, **50**). All had measurable inhibition, with IC_{50} ranging from 1.7-9.1 μ M. The two most potent compounds, **32** and **50**, had comparable enzymatic and cellular potencies as well as logD values (Table 2). They were also comparable in terms of predicted metabolic stability based on liver microsome and mouse plasma protein binding (Table 3). Being smaller in size, **32** had a

higher ligand efficiency than **50** (0.35 vs. 0.29). Also **32** was twice as permeable as **50** in MDCK assay (Table 3). Given its potency against LDHA, in vitro PK profile as well as a binding mode distinct from our previous lead compounds,⁷ **32** was selected for in vivo PK evaluation in mice. This molecule presented a low hepatic clearance (Cl_p), which we attributed at least partly to high protein-binding. It had a half-life of 2.81h, almost triple of that for our previous hydroxylactam lead,⁷ and good oral bioavailability when dosed at 5 mg/kg (Table 4, Figure S2A). At higher oral doses ranging from 50 to 200 mg/kg, **32** displayed increasing exposure (Table 4, Figure S2B) confirming its potential as a tool compound for in vivo efficacy studies in mice.

Table 3. Permeability, Metabolic Stability and Mouse Protein Binding of 32 and 50

Ex	MDCK ^a P _{app}		Liver Microsome Cl _{hep}			Mouse Plasma Protein Binding (%)
	A:B (10 ⁻⁶ cm/s)	Ratio (B:A/A:B)	Human	Rat	Mouse	
32	4.6	2.6	14	23	54	99.9
50	2.2	3.1	13	20	66	99.9

^aThe MDCK assay¹⁵ was used as an indicator of cell permeability.

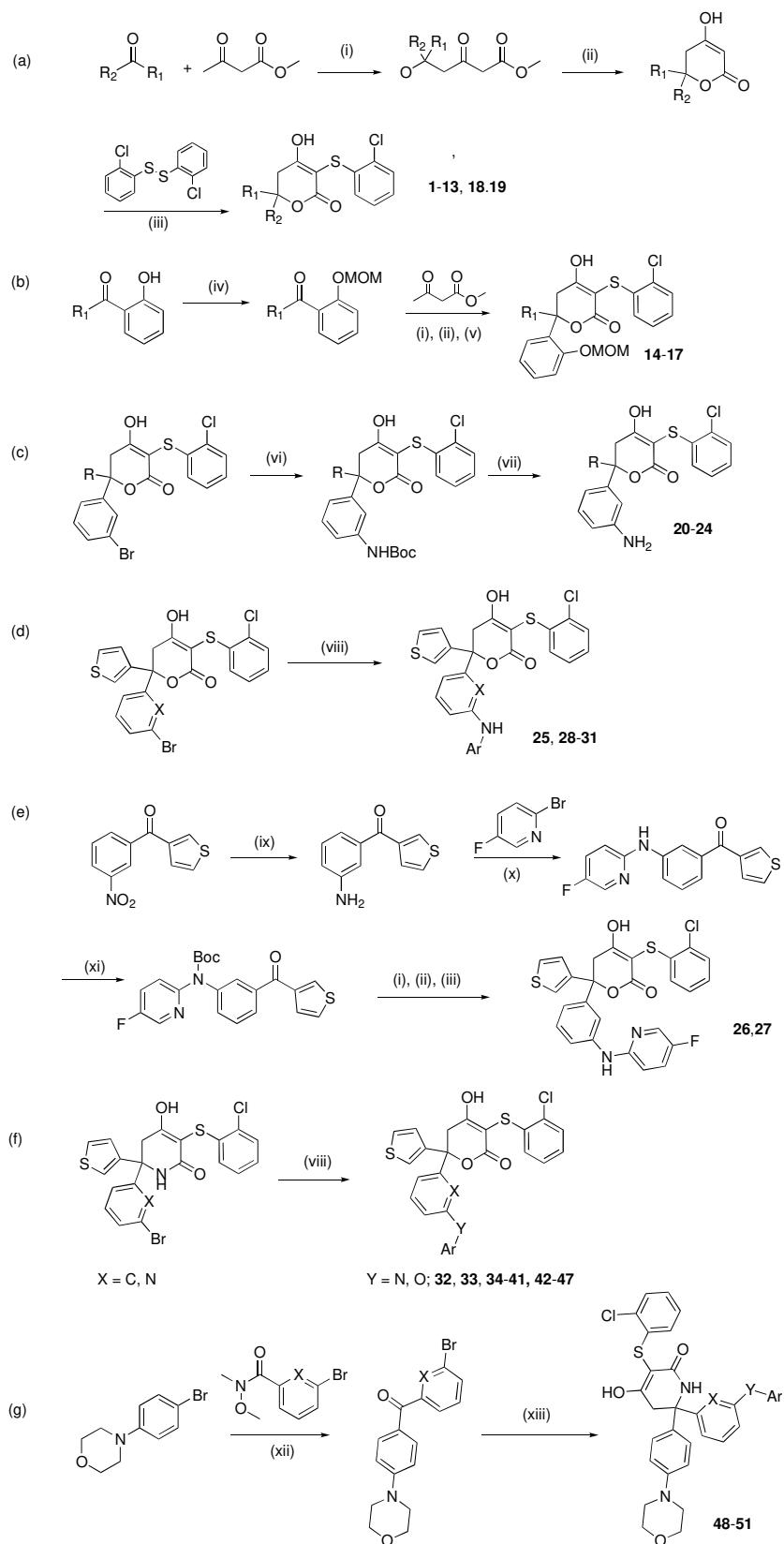
Table 4. Pharmacokinetic Parameters Following IV and PO Administrations of 32 to Mice

Route	Dose (mg/kg)	AUC (μM·h)	C _{max} (μM)	F (%)	T _{1/2} (h)	V _{ss} (L/kg)	Cl _p (mL/min/kg)
iv	1	6.5	7.36		2.81	0.671	4.89
po	5	19.4	5.95	59.5			
po	50	71.2	23.3				
po	100	235	66.9				
po	200	411	117				

We next set out to test the in vivo efficacy of **32**. MIA PaCa-2-tumor-bearing mice were dosed b.i.d at 200 and 400 mg/kg with **32** for 28 days. Although **32** was well tolerated as measured by body weight change, unfortunately no significant tumor growth inhibition was observed at either dose (SI, fig S5A). This suggested to us that the exposure of **32** was insufficient to sustain the LDH inhibition required for efficacy in the duration of the study.

The LDH inhibitors discussed above were synthesized as shown in Scheme 1a – 1g (see SI for experimental details).

Scheme 1.



Reagents and conditions for Scheme 1a - 1g : (i) NaH, BuLi, THF, 0 °C, 2h; (ii) potassium carbonate, MeOH, heat 2 h; (iii) potassium carbonate, ACN, 80 °C, 1-2 h; (iv) MOMCl, DIPEA, THF, 25 °C, 18h; (v) HCl, MeOH, 25 °C, 2h; (vi) BocNH₂, Brettphos-Admix, NaOt-Bu, 1,4-dioxane, 110 °C, 0.5 h, microwave; (vii) TFA, DCM; (viii) ArOH or ArNH₂, Brettphos-Admix, NaOt-Bu, 1,4-dioxane, 110 °C, 0.5 h, microwave; (ix) Fe powder, NH₄Cl, EtOH; (x) Pd₂(dba)₃, XantPhos, Cs₂CO₃, 1,4-dioxane, 110 °C, 0.5 h, microwave; (xi) (Boc)₂O, THF; (xii) BuLi, THF, -78 °C; (xiii) compounds were synthesized following the scheme previously described.⁷

In summary, using structure-based design we optimized a set of 6,6-diaryl substituted dihydropyrone and hydroxylactam LDH inhibitors. Surprisingly, a small change from phenyl to pyridyl led to a new inhibitor binding mode accompanied by subtle adjustment of the active site. The optimization culminated in **32**, a cell-active hydroxylactam with low in vivo clearance and 60% bioavailability in mice. In a MiaPaca-2 tumor xenograft model, **32** did not show significant tumor growth inhibition, which led us to conclude that in vivo efficacy for an orally dosed LDH inhibitor will likely require a molecule with still higher cellular potency and/or longer half-life, or an alternative modality of inhibition. Overall **32** represents a novel, potent LDH inhibitor with an improved in vivo half-life compared to previous reports⁶⁻⁸ and may inspire future drug designs against this important therapeutic target.

Accession Codes: The X-ray crystallographic structures of compound **14**, **20**, **26**, **30**, or **32** bound to human LDHA were deposited in the PDB and their accession codes are 6MV8, 6MVA, 6BAD, 6BB3, and 6BAG, respectively.

Corresponding Authors Information: Tel: (650) 467-8283; fax: (650) 225-2061; email: Wei.BinQing@gene.com, Purkey.Hans@gene.com.

Acknowledgement:

We thank Dr. James Kiefer for assistance in PDB data deposit. We thank Drs. Krista Bowman and Jiansheng Wu and their research groups for performing protein expression and purification activities. We also thank the Genentech Small Molecule analytical group for their support. We acknowledge the use of synchrotron X-ray sources at the Advanced Light Source and the Stanford Synchrotron Radiation Lightsource supported by the Department of Energy's Office of Science under contracts DE-AC02-05CH11231 and DE-AC02-76SF00515, respectively.

Abbreviations:

LDHA, lactate dehydrogenase A; LDHB, lactate dehydrogenase B; PPB, plasma protein binding; MDCK, Madin-Darby canine kidney; AUC, area under the curve; V_{ss} , steady-state volume of distribution; $T_{1/2}$, half-life; Cl_p , plasma clearance; C_{max} , maximum concentration; F, oral bioavailability

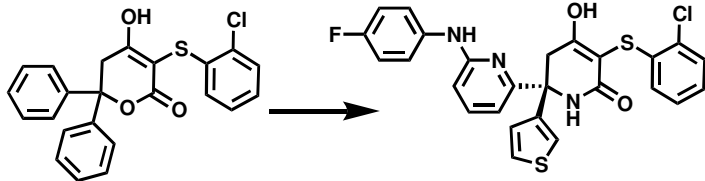
References:

- (1) Doherty, J.; Cleveland, J. Targeting Lactate Metabolism for Cancer Therapeutics. *J. Clin. Invest.* **2013**, *123* (9), 3685–3692. <https://doi.org/10.1172/JCI69741.transcription>.
- (2) Fantin, V. R.; St-Pierre, J.; Leder, P. Attenuation of LDH-A Expression Uncovers a Link between Glycolysis, Mitochondrial Physiology, and Tumor Maintenance. *Cancer Cell* **2006**, *9* (6), 425–434. <https://doi.org/10.1016/j.ccr.2006.04.023>.
- (3) Brisson, L.; Bański, P.; Sboarina, M.; Dethier, C.; Danhier, P.; Fontenille, M. J.; Van Hée, V. F.; Vazeille, T.; Tardy, M.; Falces, J.; Bouzin, C.; Porporato, P. E.; Frédérick, R.; Michiels, C.; Copetti, T.; Sonveaux, P. Lactate Dehydrogenase B Controls Lysosome Activity and Autophagy in Cancer. *Cancer Cell* **2016**, *30* (3), 418–431. <https://doi.org/10.1016/j.ccell.2016.08.005>.
- (4) McClelland, M. L.; Adler, A. S.; Shang, Y.; Hunsaker, T.; Truong, T.; Peterson, D.; Torres, E.; Li, L.; Haley, B.; Stephan, J. P.; Belvin, M.; Hatzivassiliou, G.; Blackwood, E. M.; Corson, L.; Evangelista, M.; Zha, J.; Firestein, R. An Integrated Genomic Screen Identifies LDHB as an Essential Gene for Triple-Negative Breast Cancer. *Cancer Res.* **2012**, *72* (22), 5812–5823. <https://doi.org/10.1158/0008-5472.CAN-12-1098>.
- (5) Rani, R.; Kumar, V. Recent Update on Human Lactate Dehydrogenase Enzyme 5 (*h* LDH5) Inhibitors: A Promising Approach for Cancer Chemotherapy. *J. Med. Chem.* **2015**, *5*, 150904124019006. <https://doi.org/10.1021/acs.jmedchem.5b00168>.
- (6) Billiard, J.; Dennison, J. B.; Briand, J.; Annan, R. S.; Chai, D.; Colón, M.; Dodson, C. S.; Gilbert, S. A.; Greshock, J.; Jing, J.; Lu, H.; McSurdy-Freed, J. E.; Orband-Miller, L. A.; Mills, G. B.; Quinn, C. J.; Schneck, J. L.; Scott, G. F.; Shaw, A. N.; Waitt, G. M.; Wooster, R. F.; Duffy, K. J. Quinoline 3-Sulfonamides Inhibit Lactate Dehydrogenase A and Reverse Aerobic Glycolysis in Cancer Cells. *Cancer Metab.* **2013**, *1* (1), 19. <https://doi.org/10.1186/2049-3002-1-19>.
- (7) Purkey, H. E.; Robarge, K.; Chen, J.; Chen, Z.; Corson, L. B.; Ding, C. Z.; DiPasquale, A. G.; Dragovich, P. S.; Eigenbrot, C.; Evangelista, M.; Fauber, B. P.; Gao, Z.; Ge, H.; Hitz, A.; Ho, Q.; Labadie, S. S.; Lai, K. W.; Liu, W.; Liu, Y.; Li, C.; Ma, S.; Malek, S.; O'Brien, T.; Pang, J.; Peterson, D.; Salphati, L.; Sideris, S.; Ultsch, M.; Wei, B.; Yen, I.; Yue, Q.; Zhang, H.; Zhou, A. Cell Active Hydroxylactam Inhibitors of Human Lactate Dehydrogenase with Oral Bioavailability in Mice. *ACS Med. Chem. Lett.* **2016**, *7* (10), 896–901. <https://doi.org/10.1021/acsmedchemlett.6b00190>.
- (8) Rai, G.; Brimacombe, K. R.; Mott, B. T.; Urban, D. J.; Hu, X.; Yang, S.-M.; Lee, T. D.; Cheff, D. M.; Kouznetsova, J.; Benavides, G. A.; Pohida, K.; Kuenstner, E. J.; Luci, D. K.; Lukacs, C. M.; Davies, D. R.; Dranow, D. M.; Zhu, H.; Sulikowski, G.; Moore, W. J.; Stott, G. M.; Flint, A. J.; Hall, M. D.; Darley-Usmar, V. M.; Neckers, L. M.; Dang, C. V.; Waterson, A. G.; Simeonov, A.; Jadhav, A.; Maloney, D. J. Discovery and Optimization of Potent, Cell-Active Pyrazole-Based Inhibitors of Lactate Dehydrogenase (LDH). *J. Med. Chem.* **2017**, *60* (22), 9184–9204. <https://doi.org/10.1021/acs.jmedchem.7b00941>.
- (9) Christov, P. P.; Kim, K.; Jana, S.; Romaine, I. M.; Rai, G.; Mott, B. T.; Allweil, A. A.;

- Lamers, A.; Brimacombe, K. R.; Urban, D. J.; Lee, T. D.; Hu, X.; Lukacs, C. M.; Davies, D. R.; Jadhav, A.; Hall, M. D.; Green, N.; Moore, W. J.; Stott, G. M.; Flint, A. J.; Maloney, D. J.; Sulikowski, G. A.; Waterson, A. G. Optimization of Ether and Aniline Based Inhibitors of Lactate Dehydrogenase. *Bioorg. Med. Chem. Lett.* **2021**, *41*, 127974. <https://doi.org/10.1016/J.BMCL.2021.127974>.
- (10) Boudreau, A.; Purkey, H. E.; Hitz, A.; Robarge, K.; Peterson, D.; Labadie, S.; Kwong, M.; Hong, R.; Gao, M.; Del Nagro, C.; Pusapati, R.; Ma, S.; Salphati, L.; Pang, J.; Zhou, A.; Lai, T.; Li, Y.; Chen, Z.; Wei, B.; Yen, I.; Sideris, S.; McClelland, M.; Firestein, R.; Corson, L.; Vanderbilt, A.; Williams, S.; Daemen, A.; Belvin, M.; Eigenbrot, C.; Jackson, P. K.; Malek, S.; Hatzivassiliou, G.; Sampath, D.; Evangelista, M.; O'Brien, T. Metabolic Plasticity Underpins Innate and Acquired Resistance to LDHA Inhibition. *Nat. Chem. Biol.* **2016**, *12* (10), 779–786. <https://doi.org/10.1038/nchembio.2143>.
- (11) Rai, G.; J. Urban, D.; T. Mott, B.; Hu, X.; Yang, S.-M.; A. Benavides, G.; S. Johnson, M.; L. Squadrito, G.; R. Brimacombe, K.; D. Lee, T.; M. Cheff, D.; Zhu, H.; J. Henderson, M.; Pohida, K.; A. Sulikowski, G.; M. Dranow, D.; Kabir, M.; Shah, P.; Padilha, E.; Tao, D.; Fang, Y.; P. Christov, P.; Kim, K.; Jana, S.; Muttill, P.; Anderson, T.; K. Kunda, N.; J. Hathaway, H.; F. Kusewitt, D.; Oshima, N.; Cherukuri, M.; R. Davies, D.; P. Norenberg, J.; A. Sklar, L.; J. Moore, W.; V. Dang, C.; M. Stott, G.; Neckers, L.; J. Flint, A.; M. Darley-Usmar, V.; Simeonov, A.; G. Waterson, A.; Jadhav, A.; D. Hall, M.; J. Maloney, D. Pyrazole-Based Lactate Dehydrogenase Inhibitors with Optimized Cell Activity and Pharmacokinetic Properties. *J. Med. Chem.* **2020**, *63* (19), 10984–11011. <https://doi.org/10.1021/acs.jmedchem.0c00916>.
- (12) Dragovich, P. S.; Fauber, B. P.; Boggs, J.; Chen, J.; Corson, L. B.; Ding, C. Z.; Eigenbrot, C.; Ge, H.; Giannetti, A. M.; Hunsaker, T.; Labadie, S.; Li, C.; Liu, Y.; Liu, Y.; Ma, S.; Malek, S.; Peterson, D.; Pitts, K. E.; Purkey, H. E.; Robarge, K.; Salphati, L.; Sideris, S.; Ultsch, M.; Vanderporten, E.; Wang, J.; Wei, B.; Xu, Q.; Yen, I.; Yue, Q.; Zhang, H.; Zhang, X.; Zhou, A. Identification of Substituted 3-Hydroxy-2-Mercaptocyclohex-2-Enones as Potent Inhibitors of Human Lactate Dehydrogenase. *Bioorganic Med. Chem. Lett.* **2014**, *24* (16), 3764–3771. <https://doi.org/10.1016/j.bmcl.2014.06.076>.
- (13) Fauber, B. P.; Dragovich, P. S.; Chen, J.; Corson, L. B.; Ding, C. Z.; Eigenbrot, C.; Labadie, S.; Malek, S.; Peterson, D.; Purkey, H. E.; Robarge, K.; Sideris, S.; Ultsch, M.; Wei, B.; Yen, I.; Yue, Q.; Zhou, A. Identification of 3,6-Disubstituted Dihydropyrones as Inhibitors of Human Lactate Dehydrogenase. *Bioorganic Med. Chem. Lett.* **2014**, *24* (24), 5683–5687. <https://doi.org/10.1016/j.bmcl.2014.10.067>.
- (14) Labadie, S.; Dragovich, P. S.; Chen, J.; Fauber, B. P.; Boggs, J.; Corson, L. B.; Ding, C. Z.; Eigenbrot, C.; Ge, H.; Ho, Q.; Lai, K. W.; Ma, S.; Malek, S.; Peterson, D.; Purkey, H. E.; Robarge, K.; Salphati, L.; Sideris, S.; Ultsch, M.; Vanderporten, E.; Wei, B.; Xu, Q.; Yen, I.; Yue, Q.; Zhang, H.; Zhang, X.; Zhou, A. Optimization of 5-(2,6-Dichlorophenyl)-3-Hydroxy-2-Mercaptocyclohex-2-Enones as Potent Inhibitors of Human Lactate Dehydrogenase. *Bioorganic Med. Chem. Lett.* **2015**, *25* (1), 75–82. <https://doi.org/10.1016/j.bmcl.2014.11.008>.
- (15) Irvine, J. D.; Takahashi, L.; Lockhart, K.; Cheong, J.; Tolan, J. W.; Selick, H. E.; Grove, J.

R. MDCK (Madin-Darby Canine Kidney) Cells: A Tool for Membrane Permeability Screening. *J. Pharm. Sci.* **1999**, *88* (1), 28–33. <https://doi.org/https://doi.org/10.1021/js9803205>.

- (16) Lin, B.; Pease, J. A Novel Method for High Throughput Lipophilicity Determination by Microscale Shake Flask and Liquid Chromatography Tandem Mass Spectrometry. *Comb. Chem. High Throughput Screen.* **2013**, *16* (10), 817–825. <https://doi.org/10.2174/1386207311301010007>.



LDHA IC_{50} : 1 μ M
No cell activity

LDHA IC_{50} : 1.6 nM
MiaPaca IC_{50} : 2 μ M
Orally bioavailable in Mice

